

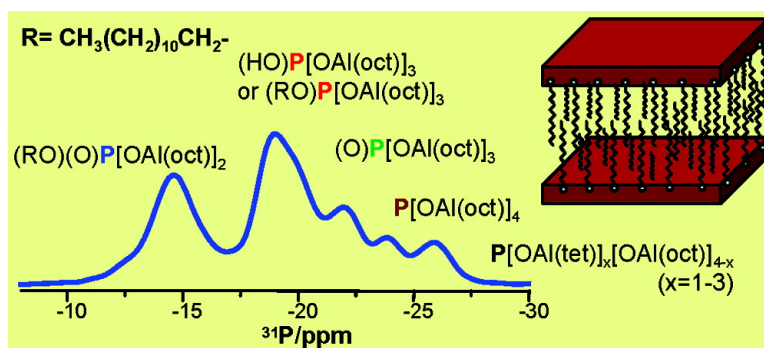
Article

Probing the Local Environments of Phosphorus in Aluminophosphate-Based Mesostructured Lamellar Materials by Solid-State NMR Spectroscopy

Yining Huang, and Zhimin Yan

J. Am. Chem. Soc., **2005**, 127 (8), 2731-2740 • DOI: 10.1021/ja040167i • Publication Date (Web): 03 February 2005

Downloaded from <http://pubs.acs.org> on March 24, 2009



More About This Article

Additional resources and features associated with this article are available within the HTML version:

- Supporting Information
- Links to the 3 articles that cite this article, as of the time of this article download
- Access to high resolution figures
- Links to articles and content related to this article
- Copyright permission to reproduce figures and/or text from this article

[View the Full Text HTML](#)



Probing the Local Environments of Phosphorus in Aluminophosphate-Based Mesostructured Lamellar Materials by Solid-State NMR Spectroscopy

Yining Huang* and Zhimin Yan

Contribution from the Department of Chemistry, The University of Western Ontario, London, Ontario, Canada N6A 5B7

Received July 7, 2004; Revised Manuscript Received November 2, 2004; E-mail: yhuang@uwo.ca

Abstract: We have characterized a series of mesostructured aluminophosphate (AIPO)-based lamellar materials by several solid-state NMR techniques. In particular, we were able to estimate the average number of Al atoms and identify the nature of other ancillary groups in the second coordination sphere for each P site. Our work has shown that a combination of several dipolar coupling-based $^{31}\text{P}/^{27}\text{Al}$ double-resonance techniques such as transfer of population in double-resonance (TRAPDOR), rotational echo double-resonance (REDOR), and heteronuclear correlation spectroscopy (HETCOR) as well as $^1\text{H} \rightarrow ^{31}\text{P}$ cross polarization (CP) can provide more detailed structural information regarding the local environments of P and Al atoms in AIPO-based mesostructured materials, which is not readily available from straightforward ^{31}P and ^{27}Al magic-angle spinning (MAS) experiments.

Introduction

Since the discovery of silicate-based mesoporous materials such as MCM-41,¹ the synthesis strategies have been extended to include aluminophosphate (AIPO)-based materials.² The AIPO-based mesostructured materials can exhibit lamellar,³ hexagonal,^{3f,4} and tubular structures.⁵ Solid-state NMR spectroscopy, in particular ^{31}P magic-angle spinning (MAS), has been extensively used to characterize the local environments of phosphorus atoms in these materials. The ^{31}P chemical shift values of the mesostructured AIPO materials are in the range 0 to -27 ppm.³⁻⁵ Usually, the starting point for the spectral assignment is to compare the observed ^{31}P chemical shifts to those reported for AIPO₄-based three-dimensional microporous materials whose ^{31}P chemical shift values normally fall in the

range -19 to -30 ppm.^{3b,6} However, it should be pointed out that in these AIPO₄-based crystalline microporous materials where the P sites usually are fully condensed, there is normally only one type of P chemical environment, that is, each P is bound to four Al atoms via bridging oxygen, $\text{P}(\text{-OAl})_4$. Thus, different ^{31}P resonances are due to crystallographically nonequivalent sites. But the situation in AIPO-based mesostructured materials is quite different. Because the degree of condensation for P atoms in these mesophases is usually low, there are many possible ^{31}P chemical environments, including $\text{P}(\text{-OAl})_{4-x}(\text{OH})_x$ ($x = 0-3$), $\text{P}(\text{-OAl})_{3-x}(\text{OH})_x(\text{OR})$ ($x = 0-2$), $\text{P}(\text{O})(\text{-OAl})_{3-x}(\text{OH})_x$ ($x = 0-2$), and $\text{P}(\text{O})(\text{-OAl})_{2-x}(\text{OH})_x(\text{OR})$ ($x = 0-1$) (with R being $\text{C}_n\text{H}_{2n+1}$ or $\text{C}_n\text{H}_{2n+1}\text{NMe}_3^+$, depending on the template used). In addition, for a given chemical environment, there may be crystallographically nonequivalent sites, provided that the materials are crystalline. In general, the ^{31}P signals can be classified into two regions.^{3b,5a} The peaks with the shift in the region -19 to -30 may be assigned to fully condensed P sites, whereas the ^{31}P resonances within the range 0 to -19 ppm are due to the P sites with lower degree of condensation. Such classification of ^{31}P signals based on chemical shift values provides an extremely useful guideline for the initial spectral assignment. However, to unambiguously determine the nature of each individual P environment in mesostructured materials requires additional information, which is not readily available from simple MAS experiments. This is because observing a ^{31}P peak in the range 0 to -19 ppm only suggests a tetrahedral P whose second coordination sphere contains less than four Al atoms. But the actual number of Al neighbors cannot be

- (1) Beck, J. S.; Vartuli, J. C.; Roth, W. J.; Leonowicz, M. E.; Kresge, C. T.; Schmitt, K. D.; Chu, C. T.-W.; Olson, D. H.; Sheppard, E. W.; McCullen, S. B.; Higgins, J. B.; Schlenker, J. L. *J. Am. Chem. Soc.* **1992**, *114*, 10834-10843.
- (2) For some reviews, see: (a) Schüth, F. *Chem. Mater.* **2001**, *13*, 3184-3195. (b) Tiemann, M.; Fröba, M. *Chem. Mater.* **2001**, *13*, 3211-3217. (c) Sayari, A.; Liu, P. *Microporous Mater.* **1997**, *12*, 149-177.
- (3) (a) Fröba, M.; Tiemann, M. *Chem. Mater.* **1998**, *10*, 3475-3483. (b) Sayari, A.; Moudrakovski, I.; Reddy, J. S.; Ratcliffe, C. I.; Ripmeester, J. A.; Preston, K. F. *Chem. Mater.* **1996**, *8*, 2080-2088. (c) Khimyak, Y. Z.; Klinowski, J. *J. Chem. Soc., Faraday Trans.* **1998**, *94*, 2241-2247. (d) Gao, Q.; Chen, J.; Xu, R.; Yue, Y. *Chem. Mater.* **1997**, *9*, 457-462. (e) Tanaka, H.; Chikazawa, M. *J. Mater. Chem.* **1999**, *9*, 2923-2927. (f) Kimura, T.; Sugahara, Y.; Kuroda, K. *Chem. Mater.* **1999**, *11*, 508-518. (g) Oliver, S.; Kuperman, A.; Coombs, N.; Lough, A.; Ozin, G. A. *Nature* **1995**, *378*, 47-50.
- (4) (a) Feng, P.; Xia, Y.; Feng, J.; Bu, X.; Stucky, G. D. *Chem. Commun.* **1997**, 949-950. (b) Zhao, X. S.; Lu, G. Q.; Whittaker, A. K.; Drennan, J.; Xu, H. *Microporous Mesoporous Mater.* **2002**, *55*, 51-62. (c) Khimyak, Y. Z.; Klinowski, J. *Phys. Chem. Chem. Phys.* **2000**, *2*, 5275-5285. (d) Kimura, T.; Sugahara, Y.; Kuroda, K. *Microporous Mesoporous Mater.* **1998**, *22*, 115-126.
- (5) (a) Luan, Z.; Zhao, D.; He, H.; Klinowski, J.; Kevan, L. *J. Phys. Chem. B* **1998**, *102*, 1250-1259. (b) Masson, N.; Pastore, H. O. *Microporous Mesoporous Mater.* **2001**, *44-45*, 173-183.

- (6) (a) Blackwell, C. S.; Patton, R. L. *J. Phys. Chem.* **1988**, *92*, 3965-3970. (b) Blackwell, C. S.; Patton, R. L. *J. Phys. Chem.* **1984**, *88*, 6135-6139. (c) Hasha, D.; Saldarriaga, L.; Hathaway, P. E.; Cox, D. F.; Davis, M. E. *J. Am. Chem. Soc.* **1988**, *110*, 2127-2135.

Table 1. Synthesis Parameters and *d* Spacings of Mesostructured AIPO Lamellar Materials

sample	gel composition ratio		surfactant concn		Al/P		<i>d</i> (nm)	
	Al(O ⁱ Pr) ₃ /H ₃ PO ₄ /C ₁₂ H ₂₅ OPO(OH) ₂		(wt %)		initial gel	solid product (EDX)	first and second phases	
MA	1.5/0/1		13		1.5	1.1	2.60	
MB	1/0/1		16		1		2.71 ^a 3.56	
MC	0.75/0/1		13		0.75		2.64 ^a 3.42	
MD	0.5/0/1		13		0.5	0.54	3.54	
ME	1/1/1		13		0.5	0.57	3.56	
MF	3/1/1		13		1.5		2.77	

^a Minor phase.

determined from a ³¹P MAS spectrum alone since the shift of the ³¹P signal to lower field can be induced by several factors other than the number of Al atoms in the second coordination sphere.^{3b,5a} A fully condensed P site can also appear at lower field outside the range -19 to -30 ppm if unusual geometry is involved. For example, one of the three fully condensed P sites in molecular sieve AIPO₄-18 resonates at -12 ppm.⁷

Recently, we have examined the local environments of different P and Al sites in a series of related AIPO-based mesostructured lamellar materials. In particular, we have employed several double-resonance solid-state NMR techniques, including ³¹P{²⁷Al} transfer of population in double-resonance (TRAPDOR), ²⁷Al{³¹P} rotational echo double-resonance (REDOR), ²⁷Al → ³¹P heteronuclear correlation spectroscopy (HETCOR), and ¹H → ³¹P cross polarization (CP). Our results show that a combination of the above-mentioned NMR techniques allows one to better characterize the P local environments.

There have been a number of reports on the synthesis of mesostructured lamellar AIPO materials.³ The particular type of lamellar material examined was prepared by using the approach described by Fröba and Tiemann,^{3a} which uses the phosphates with a long alkyl chain as template and, in some cases, as P source if no phosphoric acid is used. The reason we chose to use this particular synthetic method is because a series of mesolamellar materials with different P and Al local environments can be prepared with a wide range of Al/P ratio. Having a variety of P and Al sites in related materials allows us to demonstrate the usefulness of the NMR approaches used in differentiating different local environments. Further, the P sites in these materials have high local ordering, which yields well-defined sharp peaks in their ³¹P MAS spectra, facilitating the analysis. Some of these materials have been examined by Al K-edge X-ray adsorption spectroscopy^{3a} and NMR techniques such as ²⁷Al 3QMAS and ¹H → ³¹P HETCOR.⁸ There have also been several excellent NMR studies on other AIPO-based mesostructured materials mainly focused on ³¹P and ²⁷Al MAS,^{3b,4c,5a} ¹H → ³¹P,⁹ and ¹H → ¹³C CP.¹⁰ An ²⁷Al → ³¹P CP spectrum was also reported for a galloaluminophosphate mesoporous materials.¹¹

Experimental Section

A series of mesostructured AIPO lamellar materials were synthesized according to the literature method.^{3a} Typically, depending on the Al/P

ratio desired, a calculated amount of Al(OⁱPr)₃ (98+%, Aldrich) was combined with an aqueous solution of monododecyl phosphate (Lancaster). In some cases, phosphoric acid (85% H₃PO₄) was also added. After being stirred for 1 h at room temperature, the mixture was transferred to a Teflon-lined autoclave and heated in an oven at 393 K for 24 h. The product was then filtered, washed with ethanol, and then dried at room temperature under a vacuum. A more detailed description on synthetic procedures can be found in ref 3a. All the measurements were carried out on as-made materials. The identities of the products were confirmed by powder X-ray diffraction (XRD). The energy-dispersive X-ray (EDX) analysis was also performed to obtain Al/P ratios for selected solid products. Table 1 summarizes the conditions for the syntheses described above.

All NMR experiments were performed on a Varian/Chemagnetics Infinityplus 400 WB spectrometer operating at a magnetic field strength of 9.4 T. The ¹H, ³¹P, and ²⁷Al resonance frequencies at this field strength are 399.9, 161.6, and 104.1 MHz, respectively. The ³¹P and ²⁷Al chemical shift values are referenced to 85% H₃PO₄ and 1 M Al-(NO₃)₃ (aq), respectively. A Varian/Chemagnetics T3 7.5-mm probe was employed to acquire all the spectra unless specified otherwise. For simple ³¹P MAS experiments, the pulse length of 3 μs was used, corresponding to a nominal 90° pulse length of 10 μs. The rf field for ¹H decoupling was approximately 60 kHz, and the pulse delay was 120 s. The ²⁷Al MAS spectra were acquired by using a conventional one-pulse sequence with a very short rf pulse of 1 μs, which corresponds to a selective 90° pulse (central transition only) of 12 μs. The pulse delay was 0.2 s. The spinning speed was typically at 6–7 kHz.

The TRAPDOR experiment is a rotor-synchronized double-resonance technique designed to measure the dipolar coupling between two unlike spins involving at least one quadrupolar nucleus.¹² It is a two-step experiment. In the ³¹P{²⁷Al} TRAPDOR experiment, a normal ³¹P spin-echo (*S*₀) is obtained first, and the second (TRAPDOR) experiment is also a spin-echo (*S*), but during the first half of the spin-echo the ²⁷Al (quadrupolar nucleus, *I* = 5/2) is continuously irradiated. Irradiation of ²⁷Al under MAS conditions results in a reduction of the ³¹P echo intensity via dipolar coupling. The TRAPDOR difference spectrum ($\Delta S = S_0 - S$) is the measure of ³¹P–²⁷Al dipolar coupling. All the TRAPDOR experiments were carried out under the identical spectrometer conditions (i.e., the rf field for Al irradiation was 63 kHz, and the spinning rate was 6.5 kHz ± 2 Hz). The pulse delay was 120 s. Similar to the TRAPDOR experiment, the ²⁷Al{³¹P} REDOR experiment¹³ also involves two separate experiments, with the first one being the ²⁷Al spin-echo (*S*₀). During the second echo, instead of irradiating continuously, a number of 180° dephasing pulses are applied on the ³¹P channel, which prevents the dipolar coupling from being refocused at the end of each rotor cycle. If there is ³¹P–²⁷Al dipolar interaction it will cause a decrease in the ²⁷Al echo intensity in the REDOR spectrum (*S*). Again, the REDOR difference spectrum (ΔS) indicates the dipolar interactions. The spinning speed for REDOR

- (7) He, H.; Klinowski, J. *J. Phys. Chem.* **1993**, *97*, 10385–10388.
 (8) Schulz, M.; Tiemann, M.; Fröba, M.; Jäger, C. *J. Phys. Chem. B* **2000**, *104*, 10473–10481.
 (9) Khimyak, Y. Z.; Klinowski, J. *J. Phys. Chem. Chem. Phys.* **2001**, *2*, 2544–2551.
 (10) Khimyak, Y. Z.; Klinowski, J. *J. Phys. Chem. Chem. Phys.* **2001**, *3*, 616–626.
 (11) Holland, B. T.; Isbester, P. K.; Blanford, C. F.; Munson, E. J.; Stein, A. J. *Am. Chem. Soc.* **1997**, *119*, 6796–6803.

- (12) (a) Grey, C. P.; Veeman, W. S.; Vega, A. J. *J. Chem. Phys.* **1993**, *98*, 7711–7724. (b) Grey, C. P.; Vega, A. J. *J. Am. Chem. Soc.* **1995**, *117*, 8232–8242. (c) van Eck, E. R. H.; Janssen, R.; Mass, W. E. J. R.; Veeman, W. S. *Chem. Phys. Lett.* **1990**, *174*, 428–432.
 (13) (a) Gullion, T.; Schaefer, J. *J. Magn. Reson.* **1989**, *81*, 196–200. (b) Gullion, T.; Schaefer, J. *Adv. Magn. Reson.* **1989**, *13*, 57–83.

experiments was $6.5 \text{ kHz} \pm 2 \text{ Hz}$. The $^{27}\text{Al} \rightarrow ^{31}\text{P}$ HETCOR experiment is also based on heteronuclear dipolar coupling and can be used to map out the connectivity between two unlike spins.¹⁴ Because ^{27}Al is a quadrupolar nucleus, the cross polarization is complicated since the spin-locking efficiency is affected by several factors.¹⁵ The optimized strength of the ^{27}Al spin-locking field is 14 kHz, corresponding to an ^{27}Al 90° pulse length of $18 \mu\text{s}$ measured for the central transition. The spinning rate used for experiments was 6.5 kHz. The $^{27}\text{Al} \rightarrow ^{31}\text{P}$ CP experimental optimization was carried out using crystalline molecular sieve VPI-5. A contact time of 1 ms was used. The pulse delay was 200 ms. For $^1\text{H} \rightarrow ^{31}\text{P}$ CP experiments, the Hartmann–Hahn matching conditions were calibrated on the sample of ammonium dihydrogen phosphate. Proton 90° pulse lengths were typically $5\text{--}8 \mu\text{s}$, and a pulse delay of 5 s was used. The spin–lattice relaxation times in the rotating frame of reference for ^{31}P ($T_{1\rho}^{\text{P}}$) and ^1H ($T_{1\rho}^{\text{H}}$) spins were measured by variable spin-locking time experiments. The ^{27}Al triple quantum (3Q) MAS experiments were performed by using a Varian/Chemagnetic 4-mm T3 probe. The 3QMAS spectra were obtained by using a three-pulse, z -flier sequence.¹⁶ The rf strengths of the first two hard pulses and the third soft pulse were individually optimized, and the optimized pulse lengths were 3.8, 1.47, and $12.5 \mu\text{s}$ for the three consecutive pulses. The spinning rate was 15 kHz. All NMR spectra were acquired at room temperature. Quadrupolar parameters of various Al sites for selected samples were extracted from ^{27}Al 3QMAS spectra and simulations of the ^{27}Al MAS spectra (Supporting Information Table S1). Simulations of MAS spectra were carried out with the WSOLIDS software package provided by Prof. R. E. Wasylshen (University of Alberta).

Powder X-ray diffraction patterns were recorded on a Rigaku diffractometer using Co K α radiation ($\lambda = 1.7902 \text{ \AA}$) in a 2θ range of $5\text{--}65^\circ$ with a step-width of 0.05. The EDX analysis was performed on a LEO440 scanning electron microscope equipped with a Quartz Xone EDX analysis system.

Results and Discussion

Figure 1 shows the XRD patterns of several materials prepared by using monododecyl phosphate with different initial Al/P ratios. For samples MA–MD, since no phosphoric acid was employed, monododecyl phosphate acts as both P source and structure directing agent. The XRD patterns indicate that samples MA and MD prepared with a high (1.5 for MA) and a low (0.5 for MD) initial Al/P ratio both have lamellar structure and are X-ray pure, but they have different d spacing (Table 1). Samples MB and MC made with initial Al/P ratios between 1.5 and 0.5 appear to be a mixture of MA and MD. Although these materials all have lamellar structure, their ^{31}P and ^{27}Al MAS spectra (Figure 2) look distinctly different, clearly indicating that they have very different phosphorus and aluminum local environments. The aim of the present study is to obtain more detailed information on the local environments of P and Al atoms of these materials.

Sample MA. The ^{31}P and ^{27}Al MAS spectra (Figure 2) are similar to those reported by Schulz et al.⁸ The ^{27}Al MAS spectrum exhibits a profile with three maximums at +7, –9, and –19, with a shoulder at –24 ppm. A simulated ^{27}Al MAS and an ^{27}Al 3QMAS spectrum (Supporting Information Figure S1) show clearly that these maximums are indeed due to four separate Al sites. The peaks at –9, –19, and –24 ppm may be assigned to the octahedral Al sites on the basis of their shift

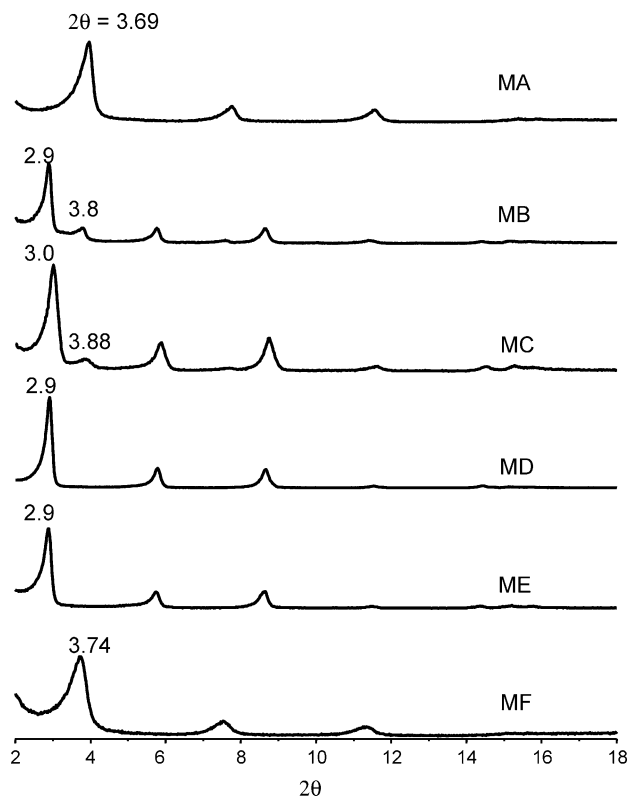


Figure 1. Powder XRD patterns of as-synthesized mesoporous AIPO materials.

values.^{3b} Although the octahedral Al atoms in AIPO₄-based three-dimensional microporous materials are always linked to four P atoms and two water molecules $[\text{Al}(-\text{OP})_4(\text{OH}_2)_2]$, the $\text{Al}(-\text{OP})_6$ environment has recently been found to exist in the two-dimensional layered aluminophosphate materials. Tuel et al. reported that the shift of such an Al environment is at around –18 ppm at a field strength of 9.4 T.¹⁷ Therefore, the exact nature of these octahedral Al sites cannot be unambiguously identified without further experiments. The assignment of the resonance at +7 ppm is also ambiguous because the shift value implies that this Al could be due to either the octahedral Al in unreacted alumina or five-coordinated Al in an AIPO phase. The ^{31}P MAS spectrum contains two sharp signals at –9.7 and –11.2 ppm. These chemical shifts may correspond to several possible P chemical environments. (1) On the basis of the discussion earlier, they may be assigned to the P sites that are not fully condensed in an AIPO phase, that is, the number of Al in the second coordination sphere is less than four. However, the chemical shift value alone gives no indication on the actual number of Al neighbors attached to a P site. (2) The chemical shifts might also indicate the existence of the P–O–P linkages.¹⁸ It is known that the phosphate-based lamellar structures do form under similar reaction conditions even in the absence of aluminum.^{3b} (3) As mentioned earlier, although a vast majority of fully condensed P sites in AIPO₄-based microporous materials exhibit chemical shifts in the range –19 to –31 ppm, the

(14) Fyfe, C. A.; Mueller, K. T.; Grondey, H.; Wong-Moon, K. C. *J. Phys. Chem.* **1993**, *97*, 13484–13495.

(15) Vega, A. J. *Solid State Nucl. Magn. Reson.* **1992**, *1*, 17–32.

(16) Amoureux, J.-P.; Fernandez, C.; Steuernagel, S. *J. Magn. Reson.* **1996**, *A13*, 116–118.

(17) Tuel, A.; Gramlich, V.; Baerlocher, Ch. *Microporous Mesoporous Mater.* **2001**, *47*, 217–229.

(18) (a) Jahn, E.; Mueller, D.; Richter-Mendau, J. In *Synthesis of Microporous Materials*; Occelli, M. L., Robson, H. E., Eds.; Van Nostrand Reinhold: New York, 1992; Vol. 1, p 249. (b) Nakayama, H.; Eguchi, T.; Nakamura, N.; Yamaguchi, S.; Danjyo, M.; Tshuhako, M. *J. Mater. Chem.* **1997**, *7*, 1063–1066.

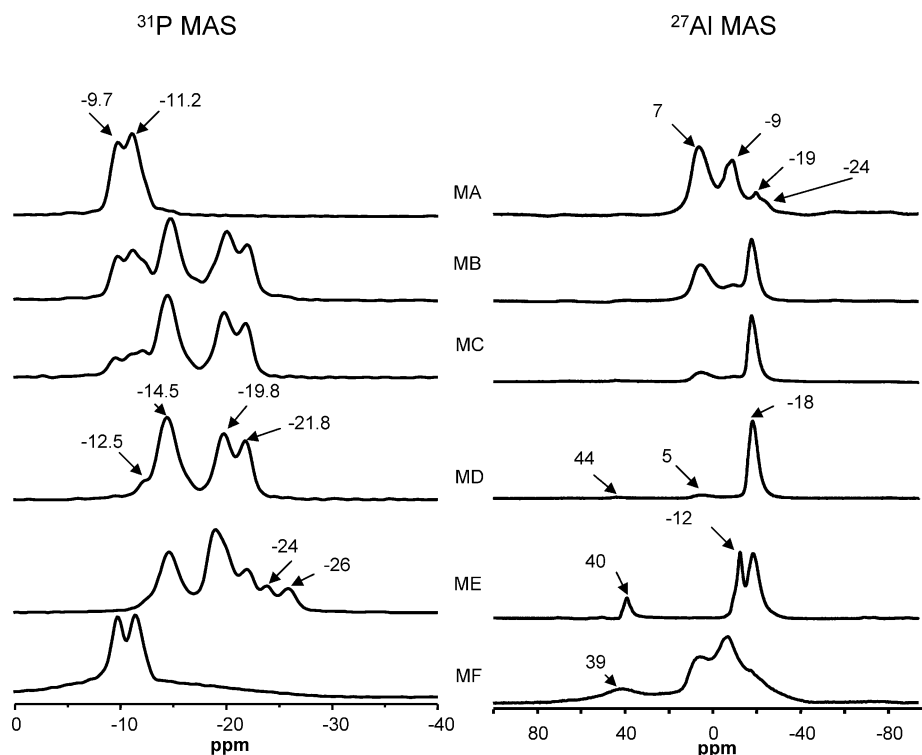


Figure 2. ^{31}P and ^{27}Al MAS spectra of as-synthesized mesostructured AIPO materials.

$\text{P}(-\text{OAl})_4$ environment does give rise to peaks at a lower field outside the above-mentioned range. Thus, the possibility that the ^{31}P signals observed in sample MA are due to fully condensed P sites cannot be completely ruled out without additional experiments. To clarify the ambiguities, we have used several double-resonance techniques.

We first carried out the $^{27}\text{Al}\{^{31}\text{P}\}$ REDOR experiments to probe the possible P–O–Al linkages for four Al sites seen in the ^{27}Al MAS spectrum. Selected ^{27}Al spin-echo (S_0), REDOR (S), and REDOR difference (ΔS) spectra with different dephasing times are shown in Supporting Information Figure S2. In each set of the spectra, both ^{27}Al spin-echo and REDOR spectra exhibit the same four Al signals. However, there is a significant decrease in the peak intensity for the -9 , -19 , and -24 ppm peaks, whereas the intensity of the $+7$ ppm resonance remains unchanged. This can be seen more clearly from REDOR difference spectra, which contain only the Al signals at -9 and -19 together with the shoulder at -24 ppm, suggesting that the AIPO layer only has three octahedral Al sites. The fact that the strong peak at $+7$ ppm seen in the ^{27}Al MAS spectrum did not appear in the REDOR difference spectra with either a short or a long dephasing time indicates that this Al experiences neither short- nor long-range dipolar interaction with any P, which suggests unambiguously that it is due to unreacted amorphous alumina with no P atom nearby. To distinguish two possible chemical environments, $\text{Al}(-\text{OP})_4(\text{OH}_2)_2$ and $\text{Al}(-\text{OP})_6$, we further examined the REDOR curves (Figure 3), which are the plots of REDOR fraction ($\Delta S/S_0$) vs dephasing time. It is well-established that for several related heteronuclear dipolar coupling-based double-resonance techniques including REDOR, TRAPDOR, and REAPDOR (rotational echo adiabatic passage double-resonance), in multiple-spin (IS_n) systems such as ours, the initial parts of the $\Delta S/S_0$ vs evolution time plots only depend on the strength of I – S dipolar interaction (i.e., the number of S

spins and internuclear I – S distances) and are independent of the exact geometry involved.^{19–21} Figure 3A shows that the REDOR curvature of the octahedral sites at -9 , -19 , and -24 ppm is very similar, especially the initial part with short dephasing times, suggesting that these Al sites experience the same magnitude of dipolar interaction with neighboring P atoms. It has been recognized that in aluminophosphate-based materials, including molecular sieves and glasses, the Al–O–P distance usually varies little.²⁰ Therefore, in the literature the difference in the initial slopes of $^{27}\text{Al}/^{31}\text{P}$ TRAPDOR and REDOR curves is explained in terms of the average number of P (or Al) atoms coordinated to observing spin Al (or P).^{20–22} In the present case, the same REDOR behavior exhibited by the Al signals implies that these octahedral Al sites have the same number of P atoms in their second coordination sphere. Figure 3A also includes the REDOR curves of two Al sites in $\text{AlPO}_4\text{-5}$. $\text{AlPO}_4\text{-5}$ is a three-dimensional microporous material and known to have a tetrahedral site, $\text{Al}(-\text{OP})_4$, at $+35$ ppm and an octahedral Al site, $\text{Al}(-\text{OP})_4(\text{OH}_2)_2$, at -13 ppm.²³ The fact that both sites have a similar initial slope supports the argument that the initial slope mainly depends on the number of P atoms in the neighborhood, rather than the geometry. Figure 3B illustrates that the initial slopes of three Al sites in sample MA are very close to those of the Al sites in $\text{AlPO}_4\text{-5}$, implying that these octahedral Al sites have four P nuclei in the second coordination sphere. This is consistent with the result reported by Chan and

- (19) (a) Bertmer, M.; Eckert, H. *Solid State Nucl. Magn. Reson.* **1999**, *15*, 139–152. (b) van Wullen, L.; Muller, U.; Jansen, M. *Chem. Mater.* **2000**, *12*, 2347–2352. (c) Chan, J. C. C.; Bertmer, M.; Eckert, H. *J. Am. Chem. Soc.* **1999**, *121*, 5238–5248. (d) Ba, Y.; He, J.; Ratcliffe, C. I.; Ripmeester, J. A. *J. Am. Chem. Soc.* **1999**, *121*, 8387–8388.
- (20) van Eck, E. R. H.; Kentgens, A. P. M.; Kraus, H.; Prins, R. *J. Phys. Chem.* **1995**, *99*, 16080–16086.
- (21) Gougeon, R. G.; Bodart, P. R.; Harris, R. K.; Kolonia, D. M.; Petrakis, D. E.; Pomonis, P. *J. Phys. Chem. Chem. Phys.* **2000**, *2*, 5286–5292.
- (22) Chan, J. C. C.; Eckert, H. *J. Magn. Reson.* **2000**, *147*, 170–178.
- (23) Fyfe, C. A.; Wong-Moon, K. C.; Huang, Y. *Zeolites* **1996**, *16*, 50–55.

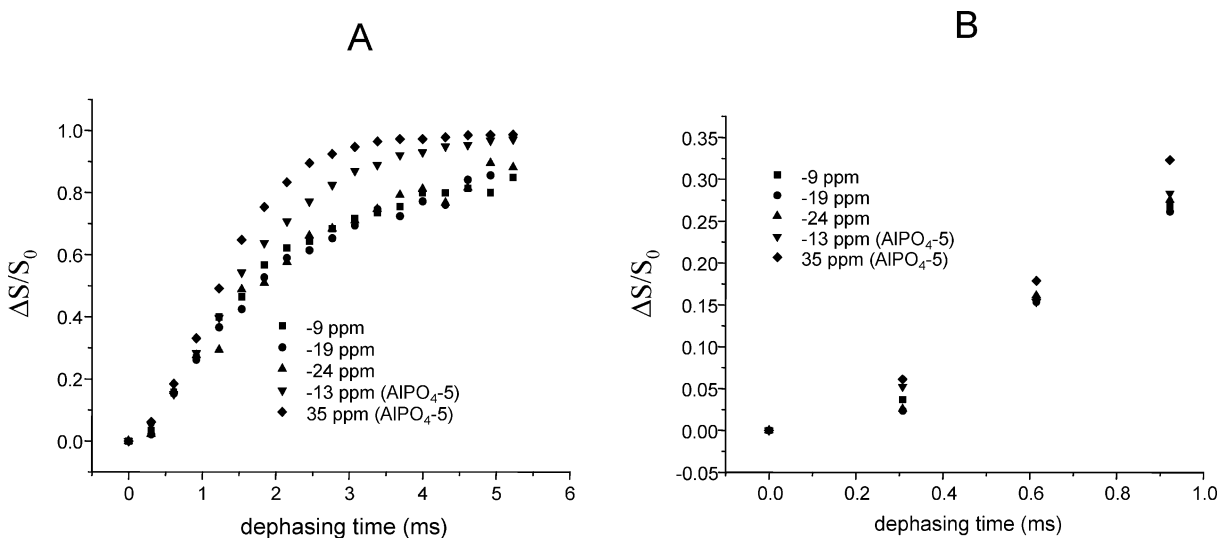


Figure 3. (A) $^{27}\text{Al}\{^{31}\text{P}\}$ REDOR fraction ($\Delta S/S_0$) as a function of dephasing time for sample MA and AIPO₄₋₅. (B) REDOR fraction of AIPO₄₋₅ and sample MA with short dephasing times to show the initial behavior.

Eckert²² that the initial slope of the REDOR curve of the Al(−OP)₆ site in Al(PO₃)₃ is greater than that of Al(−OP)₄ in AIPO₄₋₅. Our REDOR data indicate that all the octahedral Al sites in sample MA are connected to four P neighbors and two water molecules, Al(−OP)₄(OH₂)₂.

To see if both P sites observed in the MAS spectrum are linked to Al, we measured $^{31}\text{P}\{^{27}\text{Al}\}$ TRAPDOR spectra as a function of dephasing time. One set of TRAPDOR spectra are illustrated in Supporting Information Figure S3. Observing two ^{31}P signals in the TRAPDOR difference spectrum clearly indicates that both P sites are connected to the Al via P–O–Al linkages. To see how these P and Al sites are connected to each other, we have further obtained a two-dimensional $^{27}\text{Al} \rightarrow ^{31}\text{P}$ HETCOR spectrum (Supporting Information Figure S4). The Al peak at −9 ppm is connected to both P sites, whereas the Al site at −19 ppm is only linked to the P at −11.2 ppm. The Al signal observed at +7 ppm in the MAS spectrum does not appear in the HETCOR spectrum, further confirming the $^{27}\text{Al}\{^{31}\text{P}\}$ REDOR result that this Al is not part of the AIPO layer. Additional information on the degree of condensation for the P sites can be extracted from TRAPDOR curves. Figure 4A shows the plots of TRAPDOR fraction ($\Delta S/S_0$) vs dephasing time. The TRAPDOR curves of both P sites at −9.7 and −11.2 ppm are almost identical, especially the initial part with short dephasing times (Figure 4B), suggesting that both P sites experience the same magnitude of dipolar interaction with neighboring Al atoms. Again, assuming that the Al–O–P distances are very similar, the same TRAPDOR behavior shown by two ^{31}P signals implies that both P sites have the same number of Al atoms in their second coordination sphere. To estimate the actual number of Al atoms attached to each P atom, we further measured the TRAPDOR curves of two model compounds, VPI-5 and MgAPO-20, under the identical spectrometer conditions. VPI-5 is another AIPO₄-based microporous material. It has three crystallographically nonequivalent P sites with identical chemical environment, P(−OAl)₄ (Supporting Information Figure S5A).²⁴ The initial parts of the TRAPDOR curves of three P sites of VPI-5 are identical (Supporting Information Figure S6),

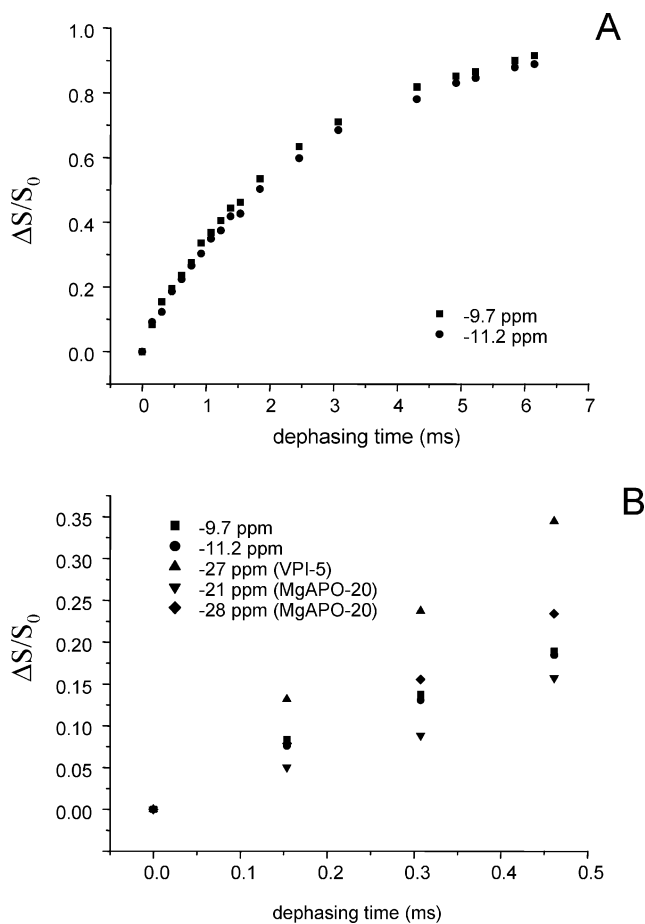


Figure 4. $^{31}\text{P}\{^{27}\text{Al}\}$ TRAPDOR experiment of sample MA. (A) TRAPDOR fraction ($\Delta S/S_0$) as a function of dephasing time. (B) TRAPDOR fraction of VPI-5, MgAPO-20, and sample MA with short dephasing times to show the initial behavior.

confirming again that the TRAPDOR curvature at short dephasing times is mainly dictated by the number of Al atoms bound to the P atom. MgAPO-20 is an aluminophosphate-based molecular sieve with SOD structure incorporated with magnesium.²⁵ Its ^{31}P MAS spectrum (Supporting Information Figure

(24) Davis, M. E.; Montes, C.; Hathaway, P. A.; Arhancet, J. P.; Hasha, D. L.; Grace, J. M. *J. Am. Chem. Soc.* **1989**, *111*, 3919–3924.

(25) Barrie, P. J.; Klinowski, J. *J. Phys. Chem.* **1989**, *93*, 5972–5974.

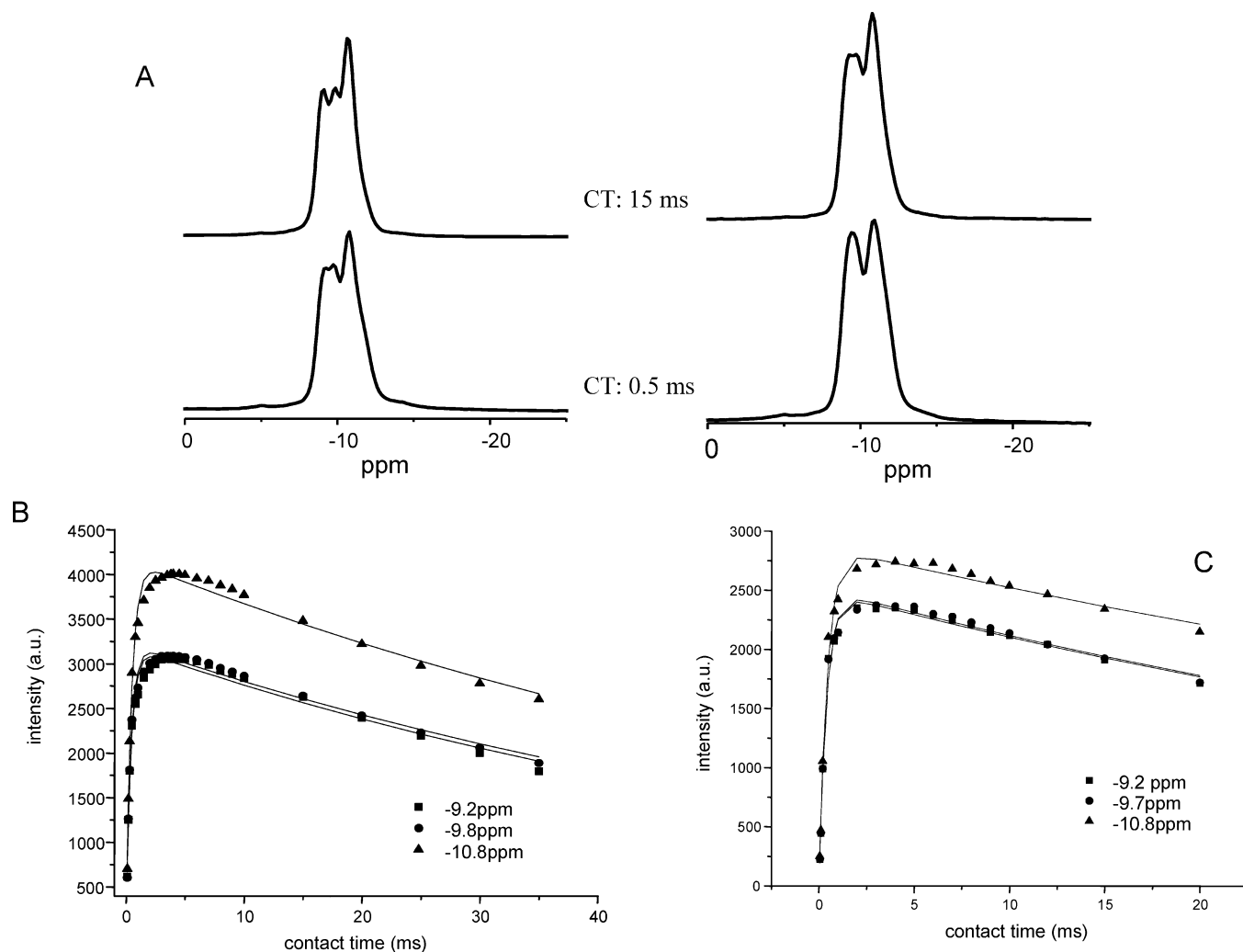


Figure 5. (A) $^1\text{H} \rightarrow ^{31}\text{P}$ spectra of sample MA before (left) and after (right) D_2O exchange. Variation of the intensities of the $^1\text{H} \rightarrow ^{31}\text{P}$ CP signals as a function of contact time (B) before and (C) after D_2O exchange.

S5B) has two ^{31}P peaks at -28 and -21 ppm, corresponding to two distinct environments of $\text{P}(\text{Mg}, 3\text{Al})$ and $\text{P}(2\text{Mg}, 2\text{Al})$, respectively. Figure 4B shows that the initial slope of the TRAPDOR curves of three known P environments in two model compounds has an order $\text{P}(\text{OAl})_4 > \text{P}(\text{OAl})_3 > \text{P}(\text{OAl})_2$. Figure 4B indicates that the initial slopes of the two P sites in sample MA are much smaller than $\text{P}(\text{OAl})_4$ in VPI-5 and in between the $\text{P}(\text{OAl})_3$ and $\text{P}(\text{OAl})_2$ in MgAPO-20 (also see Supporting Information Table S2). We were unable to perform quantitative numerical analysis of TRAPDOR data since the polar angles defining the orientation of EFG tensor of Al relative to dipolar vector required for simulation²⁶ are not known. Therefore, the number of Al atoms in the second coordination sphere for the P sites in sample MA can only be estimated at either two or three. Consequently, the possible chemical environments are (1) $(\text{RO})(\text{O})\text{P}(\text{OAl})_2$; (2) $(\text{HO})(\text{O})\text{P}(\text{OAl})_2$; (3) $(\text{HO})\text{P}(\text{OAl})_3$; (4) $(\text{O})\text{P}(\text{OAl})_3$; and (5) $(\text{RO}-)\text{P}(\text{OAl})_3$ with $\text{R} = \text{CH}_3(\text{CH}_2)_{10}\text{CH}_2-$.

The ^{13}C CP MAS spectrum (Supporting Information Figure S7) provides evidence for the existence of the $\text{CH}_3(\text{CH}_2)_{10}\text{CH}_2-$ group. The spectrum is in good agreement with that reported in the literature.⁸ On the basis of the spectral assignment by

Schulz et al., the resonance at $+65$ ppm is due to the methylene carbon in the phosphate headgroup ($-\text{CH}_2-\text{O}-\text{P}-$). Observing this and other carbons suggests that the alkyl chain is still attached to the P headgroup.

To further narrow down the possible chemical environments, we also measured the $^1\text{H} \rightarrow ^{31}\text{P}$ CP spectra as a function of contact time. Figure 5A illustrates that the resonance at -9.7 ppm seen in the MAS spectrum actually is composed of two overlapping peaks at -9.2 and -9.7 ppm. Figure 5B shows the variation of the CP signals as a function of contact time. Usually, in considering the description of $^1\text{H} \rightarrow \text{X}$ CP dynamics, the ideal CP conditions include: (1) X is a rare spin such as ^{13}C and ^{29}Si , and therefore the population ratio $\epsilon \ll 1$, (2) T_{HX} is much shorter than $T_{1\rho}^{\text{H}}$, and (3) $T_{1\rho}^{\text{X}}$ is considerably longer than $T_{1\rho}^{\text{H}}$ ($\epsilon (= N_{\text{X}}/N_{\text{H}})$ is population ratio; T_{HX} , which is related to the second moment of the dipolar interaction between H and X, is the cross polarization time constant; $T_{1\rho}^{\text{X}}$ and $T_{1\rho}^{\text{H}}$ are the X and ^1H spin-lattice relaxation time in the rotating frame of reference). In the present case, both ^1H and ^{31}P are abundant nuclei. Our measured (Supporting Information Table S3) and those reported data⁹ show that $T_{1\rho}^{\text{P}}$ can have the same order of $T_{1\rho}^{\text{H}}$. Although in the mesophases such as ours, it is difficult to evaluate the population ratios between P and H, the

(26) Kalwei, M.; Koller, H. *Solid State Nucl. Magn. Reson.* **2002**, *21*, 145–157

Table 2. ^1H to ^{31}P CP Kinetics Parameters of Sample MA

P site δ (ppm)	before D_2O exchange		after D_2O exchange	
	$T_{1\rho}^*$ (ms)	T_{HP}^* (ms)	$T_{1\rho}^*$ (ms)	T_{HP}^* (ms)
-9.2	67.0	0.42	53.9	0.41
-9.7	69.7	0.41	54.3	0.41
-11	77.8	0.47	66.9	0.45

ϵ can be very close to 1 or even much greater than unity⁹ because ^{31}P has 100% natural abundance, and the number of phosphorus atoms may be comparable to that of hydrogens in the AlPO-based materials. Since the situation is similar to that for $^1\text{H} \rightarrow ^{19}\text{F}$ in fluoropolymers, we have used the approach put forward by Harris and co-workers²⁷ and analyzed the CP data using the simple double-exponential function

$$I(\tau) = A[\exp(-\tau/T_{1\rho}^*) - \exp(-\tau/T_{\text{HP}}^*)]$$

where τ is the contact time; A is a fitting parameter for the ^{31}P signal amplitude; T_{HP}^* and $T_{1\rho}^*$ are effective parameters that characterize the increase and decrease of ^{31}P magnetization. The fitting results are given in Table 2. From Figure 5 and Table 2, it is evident that all P sites have identical CP behavior, suggesting that they experience similar proton–phosphorus dipolar interaction. It is known that in mesostructured AlPO materials, the extra framework water molecules occluded in the structure are too mobile to significantly contribute to CP processes at room temperature.⁹ Therefore, the proton sources for magnetization transfer are mainly from the organic template molecules, hydroxyl groups such as P–OH and water molecules covalently bound to octahedral Al, $\text{Al}(-\text{OP})_4(\text{OH}_2)_2$. Since the protons in hydroxyl group and water molecules coordinated to Al can be readily exchanged, we carried out D_2O exchange by stirring the sample in D_2O overnight. The fact that D_2O exchange did not cause any significant change in the CP behavior (Figure 5) and the T_{HP}^* values (Table 2) for all P sites suggests that the P sites do not have hydroxyl groups attached. Therefore, we can rule out possibilities (2) and (3). The results also suggest that the effective ^1H source for cross polarization is the methylene protons in phosphate headgroup rather than the water molecules attached to the Al, which eliminates case (4). The $^1\text{H} \rightarrow ^{31}\text{P}$ CP results indicate that the possible chemical environments are $(\text{RO})(\text{O})\text{P}(\text{OAl})_2$ and $(\text{RO}-)\text{P}(\text{OAl})_3$. The fact that the $^1\text{H} \rightarrow ^{31}\text{P}$ CP and TRAPDOR behaviors of these P sites are almost identical implies that the P sites likely differ only in their crystallographic rather than chemical environments. On the basis of the NMR results presented, we suggest that the two P peaks seen in the MAS spectrum of sample MA are due to two crystallographically nonequivalent sites with the same chemical environment of either $(\text{RO}-)\text{P}(\text{OAl})_3$ or $(\text{RO})(\text{O})\text{P}(\text{OAl})_2$. The final Al/P ratio of sample MA is close to unity. This means that if $(\text{RO}-)\text{P}(\text{OAl})_3$ represents the chemical environment, the lamellar material is electrically neutral. However, if the P atoms have $(\text{RO})(\text{O})\text{P}(\text{OAl})_2$ coordination, the layers are then negatively charged. If this is the case, the charge balancing cations are likely protons since the synthesis is carried out in an acidic solution.

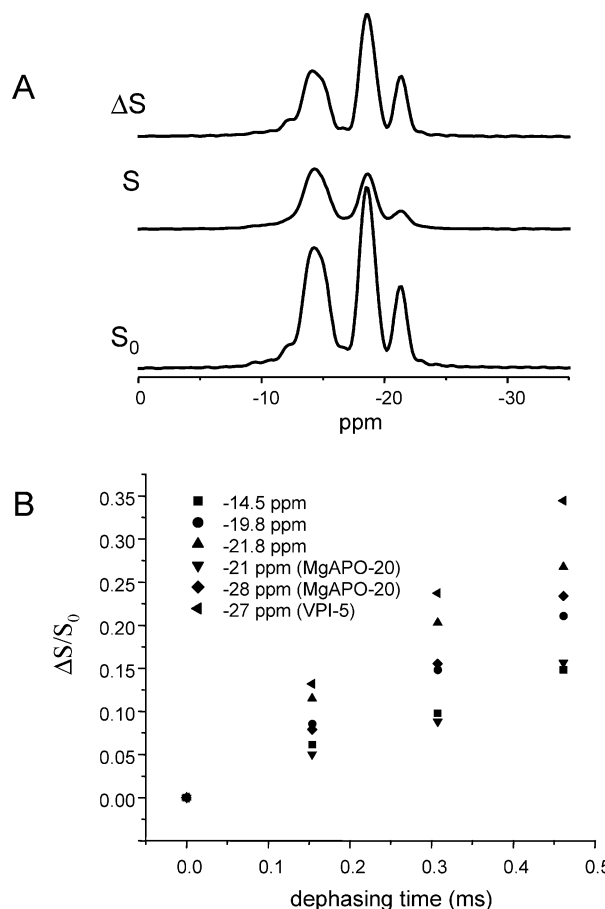


Figure 6. $^{31}\text{P}\{^{27}\text{Al}\}$ TRAPDOR of sample MD. (A) ^{31}P spin-echo (S_0), TRAPDOR (S), and TRAPDOR difference (ΔS) spectra with a dephasing time of 1.846 ms (12 rotor cycles). (B) TRAPDOR fraction as a function of dephasing time of VPI-5, MgAPO-20, and sample MD with short dephasing times.

Sample MD. This sample was prepared with a much lower initial Al/P ratio (0.5). The XRD pattern (Figure 1) indicates that it is a pure lamellar phase. The ^{27}Al MAS spectrum (Figure 2) exhibits a strong sharp peak at -18 ppm, indicating that the material has only one type of octahedral Al site. There are two small peaks at +44 and +5 ppm. The extremely weak peak at +44 ppm indicates that the AlPO layer has a negligible amount of tetrahedral Al and that the resonance at +5 ppm is due to a small amount of unreacted alumina. The ^{31}P MAS spectrum (Figure 2) contains four signals at -12.5, -14.5, -19.8, and -21.8 ppm. Again, we performed double-resonance experiments to obtain additional information regarding the local structure of various P sites. The $^{27}\text{Al}\{^{31}\text{P}\}$ REDOR curve (Supporting Information Figure S8) confirms that the Al environment is $\text{Al}(-\text{OP})_4(\text{OH}_2)_2$. Figure 6A illustrates one set of $^{31}\text{P}\{^{27}\text{Al}\}$ TRAPDOR spectra. Observation of all the P sites in the TRAPDOR difference spectrum indicates that all the P sites seen in the MAS spectrum are part of the AlPO layer and that they are all connected to the same octahedral Al at -18 ppm. From the initial slopes of TRAPDOR curves (Figure 6B and Table S2) and by comparison with the model materials, we tentatively suggest that the P sites at -12.5 (data not shown) and -14.5 ppm (Figure 6B) both have two Al neighbors, whereas the P at -19.8 ppm is attached to three Al atoms via bridging oxygen. For the P at -21.8 ppm, the average number of Al is between three and four.

(27) (a) Ando, S.; Harris, R. K.; Reinsberg, S. A. *J. Magn. Reson.* **1999**, *141*, 91–103. (b) Ando, S.; Harris, R. K.; Holstein, P.; Reinsberg, S. A.; Yamauchi, K. *Polymer* **2001**, *42*, 8137–8151. (c) Ando, S.; Harris, R. K.; Reinsberg, S. A. *Magn. Reson. Chem.* **2002**, *40*, 97–106.

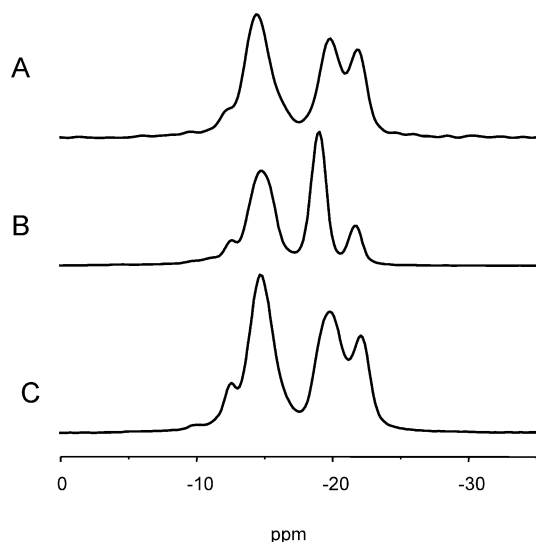


Figure 7. Sample MD: (A) ^{31}P MAS spectrum and $^1\text{H} \rightarrow ^{31}\text{P}$ CP spectra before (B) and after (C) D_2O exchange. The contact time for both spectra was 0.5 ms.

Figure 7 displays the $^1\text{H} \rightarrow ^{31}\text{P}$ CP spectra. The intensity of the peak at -19.8 ppm is significantly enhanced by the cross polarization at a short contact time (Figure 7B), suggesting that this P site has a hydroxyl group attached. Thus, the chemical environment of this site is $(\text{HO})\text{P}(-\text{OAl})_3$. It is also noticed that the relative intensity of the -21.8 ppm peak in the CP spectrum is much lower than that in the MAS spectrum. The fact that the CP discriminates against this peak implies that there are few protons around this P site acting as the source for magnetization transfer, implying that its environment is either $(\text{O})\text{P}(-\text{OAl})_3$ or $\text{P}(-\text{OAl})_4$. These assignments were further verified by performing $^1\text{H} \rightarrow ^{31}\text{P}$ CP on the same sample exchanged with D_2O . In Figure 7C, the relative intensities of the D_2O exchanged sample look much closer to those observed in the MAS spectrum. In particular, the CP no longer enhances the intensity of the P at -19.8 ppm, confirming that this P is coupled to an exchangeable proton likely in a P–OH group. The CP behavior of the ^{31}P peaks at -12.5 and -14.3 ppm are similar to that in sample MA, suggesting they are bound to an oxo group. The ^{13}C CP MAS spectrum (not shown) is almost identical to that of sample MA. All these results indicate that these two P sites have the same chemical environment: $\text{CH}_3(\text{CH}_2)_{10}\text{CH}_2-\text{O}-\text{P}(\text{O})(\text{OAl})_2$, a neutral species) count for about 51% of the total P in the layer. Considering that the final Al/P ratio is about 0.5 and assuming that the framework is neutral, the resonances at -19.8 and -21.8 ppm should both represent P species carrying a positive formal charge. As described earlier, the peak at -19.8 ppm is assigned to $(\text{HO})\text{P}(-\text{OAl})_3$, and we now suggest that the peak at -21.8 ppm is due to $\text{P}(-\text{OAl})_4$. Since the phosphate is the only source of P, the P sites at -19.8 and -21.8 ppm must result from the decomposed phosphate molecules.

The XRD pattern shows that both MA and MD have lamellar structure, but with different d spacing. Schulz et al. noticed that the short d spacing correlates with P sites with chemical shift at around -10 ppm and larger d spacing correlates with the P

sites resonating at around -20 and -24 ppm.⁸ Our data indicate that sample MD has a larger number of highly condensed P sites than that in sample MA and, consequently, the AlPO layers in sample MD must be thicker, leading to a larger d spacing. This is illustrated in Scheme 1.

Samples MB and MC. These samples were made with initial Al/P between 0.5 and 1.5. Inspection of their powder XRD patterns (Figure 1) and ^{31}P and ^{27}Al MAS spectra (Figure 2) clearly reveals that these two samples are a mixture of two different lamellar phases corresponding to samples MA and MD.

Sample ME. The initial work by Fröba and Tiemann has shown that the lamellar materials can also be prepared by using both monododecyl phosphate and H_3PO_4 .^{3a} Since the common P source for preparing AlPO materials is phosphoric acid, we also prepared several lamellar materials using a combination of H_3PO_4 and phosphate to examine how the presence of phosphoric acid during the synthesis may affect the local environments of P and Al in the mesolamellar materials.

Sample ME was made with the same initial Al/P ratio of 0.5 as sample MD. The difference is that one-half of the P source for sample ME is phosphoric acid. Its XRD (Figure 1) and ^{31}P and ^{27}Al MAS spectra (Figure 2) are in agreement with those reported in the literature.⁸ The ^{27}Al MAS spectrum exhibits three signals at $+40$, -12 , and -18 ppm. The signals at -12 and -18 ppm are due to two different octahedral Al sites. The $+40$ ppm peak originates from a tetrahedral Al site that does not exist in sample MD. It seems that H_3PO_4 promotes the formation of a tetrahedral Al site. These assignments were further confirmed by $^{27}\text{Al}\{^{31}\text{P}\}$ REDOR experiments since all three Al resonances appear in the REDOR difference spectra (Supporting Information Figure S9A,B).

In the ^{31}P MAS spectrum of sample ME, there are five major peaks at -14.7 , -19.8 , -21.8 , -24 , and -26 with relative intensities 6.4:7.2:4.0:1.0:1.4, respectively. The signals at -21.8 , -19.8 , and -14.7 ppm are also observed in the MAS spectrum of sample MD (Figure 2), and the overall appearance of the spectrum in this region also looks similar to that of sample MD except that the sample prepared using phosphoric acid has two additional high field peaks at -24 and -26 ppm. $^{31}\text{P}\{^{27}\text{Al}\}$ TRAPDOR spectra (Supporting Information Figure S9C) indicate that all the P sites are connected to Al. The number of Al atoms in the second coordination sphere were estimated via the examination of $^{31}\text{P}\{^{27}\text{Al}\}$ TRAPDOR curves (Supporting Information Figure S9D and Table S2), and they are summarized in Table 3. The results show that phosphoric acid as P source facilitates the condensation processes, yielding a larger number of fully condensed P sites. The $^{27}\text{Al} \rightarrow ^{31}\text{P}$ HETCOR experiment was also performed (spectrum not shown), and the connectivities between various Al and P sites are summarized in Table 4.

$^1\text{H} \rightarrow ^{31}\text{P}$ CP intensity of different P sites as a function of contact time is shown in Figure 8, and the corresponding values of T_{HP}^* derived from CP data are given Table 3. As mentioned earlier, the possible proton sources for CP are hydroxyl groups, phosphate headgroups, and water molecules coordinated to octahedral Al. The ^{31}P peaks at -14.7 and -19.8 ppm both have a smaller T_{HP}^* value. As pointed out by Ando et al.,²⁷ for the CP process between two abundant spins, there is not a simple approach to directly extract the true values of T_{HP} from the values of T_{HP}^* . Nonetheless, a short T_{HP}^* does indicate that CP is more effective because of the stronger dipolar interactions

Scheme 1

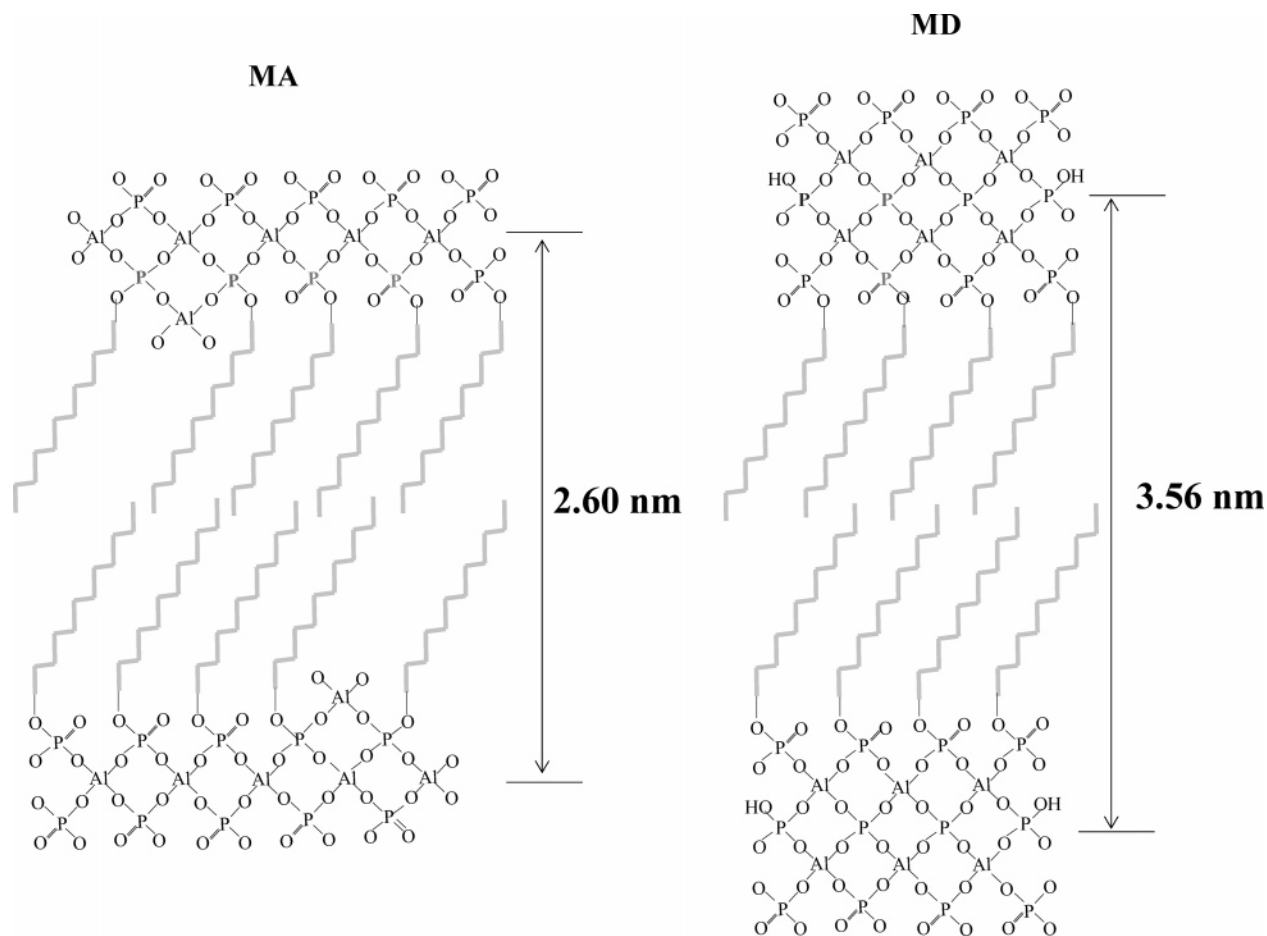


Table 3. Sample ME: The Number of Al Atoms Attached to Each P Site Estimated from $^{31}\text{P}\{^{27}\text{Al}\}$ TRAPDOR and the T_{HP}^* Values from ^1H to ^{31}P CP Experiments

^{31}P chemical shift (ppm)	-14.7	-19.8	-21.8	-24	-26
number of Al atoms	2	3	3	4	4
T_{HP}^* (ms)	0.22	0.25	0.31	0.31	0.71

Table 4. ^{27}Al -O- ^{31}P Connectivities of Sample ME

^{27}Al shift δ (ppm)	^{31}P chemical shift δ (ppm)				
	-14.7	-19.8	-21.8	-24	-26
+40					×
-12		×			
-18	×	×	×	×	×

with protons.²⁷ Therefore, the relatively short T_{HP}^* values suggest that these P sites have hydroxyl and/or phosphate headgroups. Consequently, the possible chemical environments are $(\text{AlO})_2\text{P}(\text{OR})(\text{OH})$ or $(\text{AlO})_2\text{P}(\text{OR})(\text{O})$ and $(\text{AlO})_3\text{P}(\text{OH})$ or $(\text{AlO})_3\text{P}(\text{OR})$, with R being $\text{CH}_3(\text{CH}_2)_{10}\text{CH}_2-$ for the P sites resonating at -14.7 and -19.8 ppm, respectively. The ^{31}P signal at -24 ppm has a T_{HP}^* value larger than those of the P sites at lower field. Since this P site is fully condensed (Table 3), the protons of the water molecules coordinated to octahedral Al sites are likely the main source for polarization transfer. These protons are further away from the P compared to the protons in hydroxyl and phosphate headgroups, resulting in a larger T_{HP}^* value. The fact that the -21.8 ppm resonance has the same T_{HP}^* value as the peak at -24 ppm infers that the

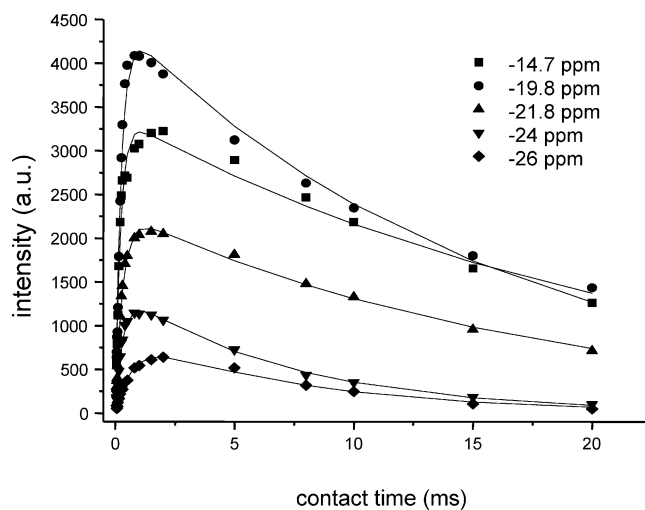


Figure 8. ^1H \rightarrow ^{31}P CP signals as a function of the contact time for sample ME.

local structure of -21.8 ppm peak is $(\text{O})\text{P}(-\text{OAl})_3$. It is interesting to note that the P resonance at -26 ppm, which is also fully condensed, has a T_{HP}^* value significantly larger than that of the -24 ppm peak. The ^{27}Al \rightarrow ^{31}P HETCOR result (Table 4) shows that this P site is connected to both octahedral and tetrahedral Al. Unlike octahedral Al, tetrahedral Al in $\text{Al}(-\text{OP})_4$ environment does not have coordinated water molecules. Therefore, the number of protons from the water molecules bound to octahedral Al available for CP is less than that from

the site at -24 ppm (which is only connected to octahedral Al), leading to a weaker dipolar interaction.

To summarize the above discussion, the peaks at -26 , -24 , and -21.8 ppm were assigned to $\text{P}[\text{OAl}(\text{tet})]_x[\text{OAl}(\text{oct})]_{4-x}$ ($x = 1-3$), $\text{P}[\text{OAl}(\text{oct})]_4$, and $(\text{O})\text{P}[\text{OAl}(\text{oct})]_3$, respectively, where Al(tet) and Al(oct) correspond to tetrahedral and octahedral sites. The resonance at -19.8 ppm is due to either $(\text{HO})\text{P}[\text{OAl}(\text{oct})]_3$ or $(\text{RO})\text{P}[\text{OAl}(\text{oct})]_3$. Assuming that the lamellar framework is neutral and taking into consideration of the Al/P ratio, we tentatively assign the resonance at -14.7 ppm to $(\text{RO})(\text{O})\text{P}[\text{OAl}(\text{oct})]_2$.

Sample MF. The initial Al/P ratio of 1.5 for preparation of this sample was the same as that for sample MA with half of the P source being phosphoric acid. The XRD pattern looks very similar to that of sample MA (Figure 1), implying that the same lamellar structure was produced. The ^{31}P MAS spectrum is also very similar to that of sample MA in that it displays two relatively sharp peaks at -9.7 and -11.2 ppm (Figure 2), indicating that the P sites in both materials have similar local environments. The only difference is that the spectrum of sample MF contains an extremely broad base with a breadth of about 40 ppm, suggesting that there is an amorphous material coexisting with the lamellar phase. The ^{27}Al MAS spectrum of sample MF has a tetrahedral Al at $+39$ ppm and three overlapping signals at $+6$, -11 , and -21 ppm. The overall appearance of three overlapping signals at higher field bears similarity to that of sample MA. The Al peak at $+39$ ppm is rather broad, indicating that the tetrahedral Al belongs to the amorphous material. The $^{27}\text{Al}\{^{31}\text{P}\}$ REDOR spectra (Supporting Information Figure S10A) show that the tetrahedral Al site is connected to the P. Similar to sample MA, the resonance at $+6$ ppm does not show up in the REDOR difference spectra, suggesting that it is due to unreacted alumina, and the peaks at -11 and -21 ppm peaks are part of the AIPO phase. In addition to the two sharp P sites, the very broad P amorphous profile also appears in the $^{31}\text{P}\{^{27}\text{Al}\}$ TRAPDOR difference spectrum (Supporting Information Figure S10B), implying that this amorphous material is AIPO in nature. All these results indicate that in sample MF, two AIPO phases coexist: one is the mesostructured AIPO lamellar phase with P and Al local structures similar to those in sample MA, and the second phase is an amorphous AIPO phase, resulting from the reaction of phosphoric acid with excess Al.

Summary

We have evaluated the local chemical environments of P and Al in a series of mesostructured AIPO lamellar materials

prepared using monododecyl phosphate as both template and phosphorus source, including the average number of Al atoms and the nature of other groups in the second coordination sphere for each P site. For example, the sample prepared with an initial Al/P of 1.5 (sample MA) contains two crystallographically nonequivalent P sites with the same chemical environments of either $\text{CH}_3(\text{CH}_2)_{10}\text{CH}_2\text{-O-P}(\text{OAl})_3$ or $\text{CH}_3(\text{CH}_2)_{10}\text{CH}_2\text{-O-P}(\text{O})(\text{OAl})_2$. For the sample synthesized with an initial Al/P ratio of 0.5 (sample MD), there are three major P sites with different chemical environments: $\text{CH}_3(\text{CH}_2)_{10}\text{CH}_2\text{-O-P}(\text{O})(\text{OAl})_2$, $(\text{HO})\text{P}(-\text{OAl})_3$, and $\text{P}(\text{OAl})_4$. Sample ME made by using both monododecyl phosphate and H_3PO_4 exhibits several different P coordination environments, including $\text{P}[\text{OAl}(\text{tet})]_x[\text{OAl}(\text{oct})]_{4-x}$; $\text{P}[\text{OAl}(\text{oct})]_4$; $(\text{O})\text{P}[\text{OAl}(\text{oct})]_3$; $\text{CH}_3(\text{CH}_2)_{10}\text{CH}_2\text{-O-P}(\text{O})[\text{OAl}(\text{oct})]_2$; $(\text{HO})\text{P}[\text{OAl}(\text{oct})]_3$; or $(\text{RO})\text{P}[\text{OAl}(\text{oct})]_3$. The work shows that a combination of several dipolar coupling-based $^{27}\text{Al}/^{31}\text{P}$ double-resonance techniques such as REDOR, TRAPDOR, and HETCOR as well as $^1\text{H} \rightarrow ^{31}\text{P}$ CP can provide much more detailed information regarding the local coordination environments around P and Al atoms in AIPO-based mesostructured materials, which is not readily available from straightforward MAS experiments. Future work will focus on quantitative analysis of the results from the $^{31}\text{P}/^{27}\text{Al}$ dipolar coupling measurements using recently proposed methods.^{26,28}

Acknowledgment. Y.H. acknowledges the financial support from NSERC of Canada for a research grant and CFI for the funding for a 400 MHz solid-state NMR spectrometer. Funding from the Canada Research Chair and Primer's Research Excellence Award programs is also gratefully acknowledged. We thank Prof. R. E. Wasylshen for providing the software WSOLIDS for spectral simulation and Dr. C. Kirby for technical assistance. We would also like to thank an unknown reviewer for the insightful and critical comments.

Supporting Information Available: Additional experimental results (10 figures and three tables). This material is available free of charge via the Internet at <http://pubs.acs.org>.

JA040167I

- (28) (a) Strojek, W.; Kalwei, M.; Eckert, H. *J. Phys. Chem. B* **2004**, *108*, 7061–7073. (b) Goldbourt, A.; Vega, S.; Gullion, T.; Vega, A. *J. Am. Chem. Soc.* **2003**, *125*, 11194–11195.